



ORIGINAL ARTICLE

Detection of *TSC1/TSC2* mosaic variants in patients with cardiac rhabdomyoma and tuberous sclerosis complex by hybrid-capture next-generation sequencing

Siyu Wang^{1,2}  | Hairui Sun^{1,3}  | Jianbin Wang⁴ | Xiaoyan Gu¹ | Lu Han⁵ | Yuduo Wu^{1,5} | He Yan⁶ | Ling Han⁷ | Hongjia Zhang⁵ | Yihua He¹

¹Department of Echocardiography, Beijing An Zhen Hospital, Capital Medical University, Beijing, China

²Department of Medical Ultrasonics, Beijing Chao Yang Hospital, Capital Medical University, Beijing, China

³School of Biological Science and Medical Engineering, Beihang University, Beijing, China

⁴College of Life Science, Tsinghua University, Beijing, China

⁵Cardiac Surgery Department, Beijing An Zhen Hospital, Capital Medical University, Beijing, China

⁶Bijoux Healthcare company, Beijing, China

⁷Department of Pediatrics, Beijing An Zhen Hospital, Capital Medical University, Beijing, China

Correspondence

Yihua He, Department of Echocardiography, Beijing An Zhen Hospital, Capital Medical University, No. 2, Anzhen Road, Chaoyang District, Beijing 100029, P.R. China.
Email: yihuaheecho@163.com

Funding information

National Key R&D Program of China (grant/award number: 2018YFC1002300), Beijing Laboratory for Cardiovascular Precision Medicine, Beijing, China (grant/award number: 116211), Key Laboratory of Fetal Heart Disease Maternal and Child Medicine, Beijing, China (grant/award Number: BZ0308).

Abstract

Background: Fetal cardiac rhabdomyoma (CR) is strongly associated with tuberous sclerosis complex (TSC), which is caused by variants in *TSC1* and *TSC2*. However, in 10%–15% of patients with clinically confirmed TSC, no *TSC1/TSC2* variants are identified by panel sequencing or multiplex ligation-dependent probe amplification (MLPA).

Methods: We analyzed eight fetuses with CR and their families. No *TSC1/TSC2* variants had previously been identified for six of these fetuses, and we suspected the other two families of gonadal mosaicism. We performed next-generation sequencing (NGS) using CR tissue, umbilical cord tissue, and parental blood. All positive results, involving two paternal semen, were verified by droplet digital polymerase chain reaction (ddPCR).

Results: Four fetuses carried low-level mosaic variants (0.05%–14.89%), and two only exhibited somatic mosaic variants in the CR tissue (15.76% and 37.69%). Two fathers had gonadal mosaicism (9.07% and 4.86%). We identified nine pathogenic variants in eight fetuses, including one fetus with a second-hit variant.

Conclusion: The fetuses assessed in this study carried low-level and somatic mosaic variants, and CR tissue from one fetus exhibited a second-hit variant. Heterozygous gonadal variants can exist in patients with low-level mosaicism. Combining NGS with ddPCR improves the accuracy of prenatal TSC diagnosis.

Siyu Wang and Hairui Sun contributed equally to this work as co-first authors.

This is an open access article under the terms of the Creative Commons Attribution-NonCommercial-NoDerivs License, which permits use and distribution in any medium, provided the original work is properly cited, the use is non-commercial and no modifications or adaptations are made.

© 2021 The Authors. *Molecular Genetics & Genomic Medicine* published by Wiley Periodicals LLC

KEYWORDScardiac rhabdomyoma, hybrid-capture next-generation sequencing, mosaic variants, *TSC1/TSC2*

1 | INTRODUCTION

Tuberous sclerosis complex (TSC) is an autosomal dominant genetic disease that is caused by pathogenic variants in *TSC1* (OMIM 605284) and *TSC2* (OMIM 191092). The main clinical manifestations of TSC in patients are hamartomas in any organ, such as the skin, brain, kidneys, lungs, and heart (DiMario et al., 2015; Henske et al., 2016). *TSC1* is located on chromosome 9q34, contains 23 exons, and encodes an 8.6-kb transcript; *TSC2* is located on chromosome 16p13, contains 42 exons, and encodes a 5.5-kb transcript (European Chromosome 16 Tuberous Sclerosis C, 1993; van Slechtenhorst et al., 1997). *TSC1/TSC2* mainly regulates cell growth and differentiation, and variants of these two genes cause dysfunction of the TSC protein complex (Au et al., 1998; Jones et al., 1999; Niida et al., 1999). *TSC1/TSC2* variants enhance the mechanistic target of rapamycin (mTOR) kinase activity, which leads to uncontrolled cell differentiation and growth as well as tumorigenesis (DiMario et al., 2015). Heterozygous single nucleotide variants, indels, and duplications in all exons and intronic regions near exons in *TSC1/TSC2* can be detected by *TSC1/TSC2* panel sequencing and multiplex ligation-dependent probe amplification (MLPA) (Nellist et al., 2015). However, in 10%–15% of patients with clinically confirmed TSC, no variants can be identified by these two methods (Northrup & Krueger, 2013), these TSC patients are referred to as “no mutation identified” (NMI) (Camposano et al., 2009). In 2015, Tyburczy et al. identified *TSC1/TSC2* variants in 85% of NMI patients (45/53) using next-generation sequencing (NGS) (Tyburczy et al., 2015). Mosaic variants accounted for 58% (26 of 45) of all variants identified, and intronic variants accounted for 40% (18 of 45). The mosaic variants involved somatic variants in DNA isolated from angiofibroma biopsies and low-level mosaic variants in DNA isolated from blood or saliva. The study demonstrated that the detection rate of *TSC1/TSC2* variants can be improved by increasing the depth of sequencing and by analyzing tumor tissues.

Fetal cardiac rhabdomyoma (CR) is a predictor of TSC (Chen et al., 2019; Gu et al., 2018; Jozwiak & Kotulska, 2006; Pavlicek et al., 2021). Previous studies have assessed *TSC1/TSC2* somatic variants in angiofibromas, angiolipomas (AMLs), and lymphangioliomyomatosis (LAM) tissue (Lam et al., 2017). In 2017, Godava et al. detected a c.4861A>T variant and a large deletion in *TSC2* in a tumor tissue sample from a single giant CR (Godava et al., 2017). This was the first-ever report of sequencing analysis of CR tissue. We previously published two studies of the

correlation between fetal CR and TSC at our center. The objectives of the first study were to investigate the correlation between suspected fetal CR and TSC by *TSC1/TSC2* panel sequencing and MLPA using umbilical cord tissue and to compare the *TSC1/TSC2* genotypes of these fetuses with suspected prenatal CR phenotypes (Gu et al., 2018). We found *TSC1/TSC2* variants in 13 fetuses with multiple tumors, but no *TSC1/TSC2* variant in two fetuses with single tumors. Five of the *TSC1/TSC2* variants were predicted to be “pathogenic,” six were “likely pathogenic,” one was of “uncertain significance,” and one was “likely benign.” The second study aimed to investigate the correlation between fetal CR and TSC by autopsy and *TSC1/TSC2* panel sequencing and MLPA using umbilical cord tissue (Chen et al., 2019). The postmortem examination identified 36 subjects as having CR: 27 of the 29 fetuses with multiple CR and five of the seven fetuses with single CR exhibited *TSC1/TSC2* pathogenic variants. In the current study, we sought to identify low-level and somatic mosaic variants in NMI fetuses and to improve the accuracy of prenatal diagnosis of TSC. DNA from umbilical cord tissue, CR tissue, and parental blood for eight fetuses was analyzed by hybrid capture-based NGS to detect *TSC1/TSC2* variants. Cases 1 and 2 in this study were previously described in Chen et al., as cases 23 and 46, respectively; in both of these cases, no pathogenic *TSC1/TSC2* variants were detected in umbilical cord tissue by *TSC1/TSC2* panel sequencing or MLPA.

2 | MATERIALS AND METHODS

2.1 | Ethical compliance

Our institution's ethics committee approved this study.

2.2 | Participants

From January 2018 to May 2019, we recruited 64 pregnant women and their family members who came to the Maternal-Fetal Consultation Center for Congenital Heart Disease at the Beijing An Zhen Hospital after receiving a fetal diagnosis of CR by fetal echocardiography (FE). *TSC1/TSC2* panel sequencing and MLPA were performed sequentially on specimens from these fetuses and their parents. Using methods described previously (Chen et al., 2019; Gu et al., 2018), *TSC1/TSC2* panel sequencing was used to identify single nucleotide polymorphisms/indels located

in *TSC1*(NM_000368.4)/*TSC2*(NM_000548.3) exons and variants located in splice sites with 10 base pairs (bp) of an exon. Multiplex ligation-dependent probe amplification (MLPA) analysis was performed to identify large deletions and duplications in *TSC1/TSC2*. For more details, please see the Supplementary data online methods.

We identified *TSC1/TSC2* variants in 48 of the 64 fetuses, including small indels and point variants in 47 of the 48 fetuses and a large deletion in one of the 48 fetuses. Of the 47 indels and point variants, 29 were sporadic variants, and 18 were familial variants, with suspected gonadal mosaicism in three of the fetuses' parents, including one NMI father who was clinically diagnosed with TSC and two parents who had more than one fetus with TSC. We selected eight families for further study: six for whom no *TSC1/TSC2* variants were detected in umbilical cord tissue by *TSC1/TSC2* panel sequencing or MLPA and two in which we suspected the parents of gonadal mosaicism. Postmortem examinations had been performed for all eight fetuses, so we were able to obtain CR tissue and umbilical cord tissue, as well as parental blood, for *TSC1/TSC2* hybrid capture-based NGS. All positive results, including positive results from two paternal semen samples, were verified by droplet digital polymerase chain reaction (ddPCR). We froze all umbilical cord and CR tissue. All CR tissue samples contained solely CR tissue.

Parents who underwent genetic testing were asked to provide written informed consent, indicating that they agreed to provide blood and semen sampling for genetic testing. Pregnant women who were willing to provide fetal samples were required to provide the written consent for pathologic autopsy and genetic testing.

2.3 | Fetal echocardiography examination

We performed FE on the 64 fetuses, according to the International Society of Ultrasound in Obstetrics and Gynecology (ISUOG) guidelines (Carvalho et al., 2013), using a Voluson E8/E10 ultrasound system (GE Healthcare, Zipf, Austria) with transabdominal 2–4-MHz curvilinear transducers. We aimed to observe the CR position, number, and complication.

2.4 | Next-generation sequencing

2.4.1 | DNA extraction

The genomic DNA was extracted from the umbilical cord, seminal fluid, and parental blood using a Qiagen DNA Blood Midi/Mini kit (Qiagen GmbH).

2.4.2 | SureSelect DNA design

We designed a custom *TSC1/TSC2* capture array using the SureDesign software provided by Agilent Technologies. The design was tailored to the 150 bp paired-end sequencing technology from Illumina. The *TSC1* locus (GRCh37/hg19 chromosome 9q34: g.135828761–135757225; bases covered: 56,521 bp [79.01%]) and 61311 bases encompassing the *TSC2* locus (GRCh37/hg19 chromosome 16p13.3: g.2087455–2148765; bases covered: 50511 bp [82.39%]). To allow identifying of variants affecting promoters and other 5' regulatory elements, ~10 kilobases (kb) upstream of *TSC1/TSC2* were captured. Also, ~10 kb downstream of the *TSC1/TSC2* 3'-UTR was captured to detect variants affecting downstream regulatory sequences.

2.4.3 | Sequencing, variant annotation, filtering, and classification

We sheared the 300ng genomic DNA concentrations with Covaris LE220 Sonicator (Covaris) to target 150–200bp average size. DNA libraries were prepared using the KAPA Hyper Prep kit (KAPA). The fragments were repaired the 3' and 5' overhangs and added with "A" tail using End repair and A-Tailing Mix (a KAPA). And then ligated with xGen Dual Index UMI adapter (a member of IDT) using the DNA ligase (a component of KAPA) and purified using Agencourt AMPure XP beads (Beckman). We amplified the adapter-ligated DNA fragments with HiFi HotStart DNA Polymerase (several KAPA). Finally, the precapture libraries containing target region sequences were captured using the customized *TSC1/TSC2* capture library kit as described above.

Then, we measured the enriched sequencing libraries' DNA concentration with the Qubit 2.0 fluorometer dsDNA HS Assay (Thermo Fisher Scientific). The size distribution of the resulting sequencing libraries was analyzed using Agilent BioAnalyzer 2100 (Agilent). The libraries were used in cluster formation on an Illumina cBOT cluster generation system with HiSeq PE Cluster Kits (Illumina). Paired-end sequencing was performed using an Illumina HiSeq X Ten system following Illumina-provided protocols for 2 × 150 paired-end sequencing. Raw image files were processed using Bcl To Fastq (Illumina) for base calling and generating raw data. We generated Consensus reads with Fabio using -min-base-quality of 30 and -min-reads of 3, variant calling was performed with verdict using mapping quality (-Q) of 20 and variant reads (-r) of 2. The reads were aligned to the NCBI human reference genome (hg19/GRCh37) using the BWA. BAM files were subjected to single nucleotide polymorphism (SNP) analysis, duplication marking, indel realignment, and recalibration using GATK

TABLE 1 Fetal echocardiology characteristics of Cardiac rhabdomyoma

No	Age (years)	Gestational age (weeks)	Position	Number	Maximum diameter (mm)	Complication
1	28	28	LV, LV, IVS	3	9.6	/
2	27	32	LV	1	11.5	Tricuspid Regurgitation
3	25	25	LV	1	8.2	/
4	26	24	LV	1	5.3	/
5	35	31	LV	1	10.0	/
6	33	28	LV	1	13.0	/
7	29	20	LV, LV	2	8.0	/
8	28	24	LV, LV, RV, RV	4	10.0	/

Abbreviations: APB, Atrial premature beat; IVS, interventricular septum; LV, left ventricle; RV, Right ventricle.

and Picard. The mean and median sequencing depth on the target region was 7422.86 and 5889.71 (ranging from 1781.16 to 26658.90), respectively. After variant detection, we used ANNOVAR for annotation (<http://wannovar.wglab.org/>). Variant frequencies were determined in dbSNP150 (<https://www.ncbi.nlm.nih.gov/SNP/>), the 1000 Genomes Project (<http://www.internationalgenome.org/>), Exome Variant Server (<http://evs.gs.washington.edu/EVS/>), ExAC (<http://exac.broadinstitute.org/>), gnomAD (<http://gnomad-old.broadinstitute.org/>), and in-house database to remove common SNPs (minor allele frequency >0.1%). Then, we prioritized nonsynonymous, splicing, and frameshift, non-frameshift variants, as well as variants located in intronic and untranslated regions for study. SIFT (<http://sift.jcvi.org/>), PolyPhen-2 (<http://genetics.bwh.harvard.edu/pph2/>), variantTaster (<http://www.varianttaster.org/>), and CADD (<http://cadd.gs.washington.edu/>) were used for predicting the pathogenicity of missense variants, while Human Splicing Finder (<http://www.umd.be/HSF/>) and MaxEntScan (http://genes.mit.edu/burgelab/maxent/Xmaxent_scoreseq.html) were used for evaluating the effects on splicing. Moreover, databases such as OMIM (<http://omim.org/>), ClinVar (<http://www.ncbi.nlm.nih.gov/clinvar/>), LOVD (<http://www.lovd.nl/>), and Human Gene variant Database (<http://www.hgmd.org/>) used to determine variant pathogenicity where appropriate. We utilized the ACMG variant classification recommendations for all reported variants (Richards et al., 2015).

2.5 | Confirmation of identified variants

We performed ddPCR to confirm the detected variants. We used the QX200™ Droplet Digital™ PCR System (Bio-Rad, Hercules, CA, USA) in this study according to the manufacturer's instructions. The ddPCR reaction mixtures (20 μ L) contained 10 μ L ddPCR Supermix, 10 μ M of each primer, 10 μ M of the probe, and 5.4 μ L of the sample.

Put a Droplet Generator (DG) with an 8-channel DG8 into the holder. Then, 20 μ L of fluorescent PCR reaction mixture adds to the DG8 cartridge's middle row. We added the DG8 cartridge 70 μ L of DG oil/well in the bottom row. We transferred the droplets formed in the top row of holes in DG8 cartridge to a 96-well PCR plate (Bio-Rad). The PCR plate was subsequently heat-sealed with pierceable foil and then amplified in a T100 deep-well thermal cycler. The thermocycling protocol was initial denaturation at 95°C for 10 min, then 40 cycles of denaturation at 94°C for 30 s, annealing at 60°C for 60 s, and, finally, incubation at 98°C for 10 min and storage at 4°C. After cycling, we placed a 96-well plate into the QX200™ Droplet Reader. We analyzed the droplets of each sample sequentially and can upload data to the computer for final analysis.

3 | RESULTS

The average age of the eight pregnant women included in this study was 28.3 years (range: 24–35 years), and the average gestational age was 27.3 weeks (range: 24–34 weeks). We subjected all fetuses to FE. Five of the cases exhibited single tumors, and three had multiple tumors. One fetus had a complication related to CR (Table 1).

There were six NMI fetuses (cases 1, 2, 3, 4, 5, and 6) and two fetuses (cases 7 and 8) with *TSC1/TSC2* variants identified by hybrid-capture NGS. Four of the six NMI fetuses had low-level mosaic variants (cases 2, 3, 4, and 5), and two carried somatic mosaic variants in the CR tissue (cases 1 and 6). We identified nine pathogenic variants in eight fetuses, including one fetus with two different variants (case 5): one was in *TSC1*, and eight were in *TSC2*. These variants consisted of four splice site variants, two indels, two nonsense variants, and one missense variant (Table 2). Two of the fetuses had heterozygous variants inherited from fathers with low-level mosaicism and gonadal mosaic variants (Table 3).

TABLE 2 The NGS and ddPCR result of the umbilical cord and cardiac rhabdomyoma tissue

No	Variant	Protein change	Variant type	Refer (PMID)	NGS			ddPCR				
					UC(V/TD)	UC(AF)	CR(V/TD)	CR(AF)	UC(V/TD)	UC(AF)	CR(V/TD)	CR(AF)
1	c.4663-1G>A ^a	/	splice	11112665	0/1202	0	43/379	11.35%	0/3169	0	2034/12917	15.76%
2	c.976-5G>A ^a	/	splice	26540169	10/1817	0.55%	131/880	14.89%	24/3345	0.72%	4522/19184	23.57%
3	c.894dupT ^a	p.V299fs	indel	NV	131/995	13.17%	345/1097	31.45%	564/3788	14.89%	578/1948	29.67%
4	c.3323_3350del ^a	p.A1108fs	indel	NV	51/656	7.77%	85/357	23.81%	611/5005	12.20%	4152/11343	36.60%
5 ^c	c.475G>T ^a	p.E159*	nonsense	NV	0/1631	0	124/1645	7.54%	0/3552	0	1766/12506	14.12%
5 ^c	c.3412C>T ^a	p.R1138*	nonsense	16981987	0/1504	0	134/1570	8.49%	2/3959	0.05%	1779/11784	15.10%
6	c.1831C>T ^a	p.R611W	missense	26540169	0/1230	0	446/1459	30.57%	0/1187	0	5134/13620	37.69%
7	c.976-5G>A ^a	/	splice	26540169	715/1512	47.29%	1020/1813	56.26%	2799/5482	51.06%	7580/13831	54.80%
8	c.2356C>T ^b	p.R786*	nonsense	9242607	1393/2867	48.59%	984/2000	49.20%	1342/2696	49.78%	2397/5959	49.28%

Abbreviations: AF, allele frequency; CR, cardiac rhabdomyoma; ddPCR, droplet digital polymerase chain reaction; NGS, next-generation sequencing; NV, novel variant; UC, umbilical cord; V/TD, variant/total depth.

^aGenBank: NM_000548.4.

^bGenBank: NM_000368.4.

^cSecond-hit variant.

TABLE 3 The NGS and ddPCR result of the gonadal variants

No	Variant	Protein Change	Variant type	Refer (PMID)	NGS			ddPCR				
					PB(V/TD)	PB(AF)	PS	PB(V/TD)	PB(AF)	PS(V/TD)	PS(AF)	
7	c.976-5G>A ^a	/	splice	26540169	51/731	6.98%	NA	NA	467/5149	9.07%	5006/14642	34.19%
8	c.2356C>T ^b	p.R786*	nonsense	9242607	39/1054	3.70%	NA	NA	208/4277	4.86%	892/2462	36.23%

Abbreviations: AF, allele frequency; ddPCR, droplet digital polymerase chain reaction; NA, not available; NGS, next-generation sequencing; PB, paternal blood; PS, paternal semen; V/TD, variant/total depth.

^aGenBank: NM_000548.4.

^bGenBank: NM_000368.4.

3.1 | Low-level and somatic mosaic variants

The allele frequency (AF) of the low-level variants identified in the four NMI fetuses was <25% in the fetal umbilical cord tissue samples, and two of the mosaic variants in cases 2 and 5 had extremely low AFs (24/3345, 0.72% and 2/3959, 0.05%, respectively). The AFs were higher in the CR tissue (4522/19184, 23.57% and 1779/11784, 15.10%, respectively) than in the umbilical cord tissue (Figures 1 and 2).

For the two cases with somatic mosaic variants, the AFs in the CR tissue were 15.76% (2034/12917) and 37.69% (5134/13620), respectively, and the AFs in the umbilical cord tissue were 0% (Figure 3).

3.2 | Two variants identified in one fetus

We identified two different variants in case 5: the *TSC2* c.475G>T, p.E159* nonsense variant was detected in CR tissue (1766/12506, 14.12%), and the *TSC2* c.3412C>T,

p.R1138* nonsense variant was detected in umbilical cord tissue and CR tissue (2/3959, 0.05% and 1779/17784, 15.10%, respectively) (Figure 2).

3.3 | Variants inherited from fathers with gonadal mosaicism

Among the eight families analyzed, we identified six fetuses with sporadic variants and two that inherited variants via paternal semen (cases 7 and 8). The father of case 7 was diagnosed with TSC and had clinical manifestations such as multiple hypomelanotic macules, shagreen patches, and renal angiomyolipomas. We classified him as NMI after *TSC1/TSC2* panel sequencing and MLPA. DDPCR analysis detected a c.976-15G>A *TSC2* variant at an AF of 9.07% (467/5149) in the blood and at 34.19% (5006/14642) in the semen (Figure 4). The father of case 8 did not exhibit any TSC-related clinical manifestations and was classified as NMI after *TSC1/TSC2* panel sequencing and MLPA. DDPCR analysis detected a c.2356C>T,

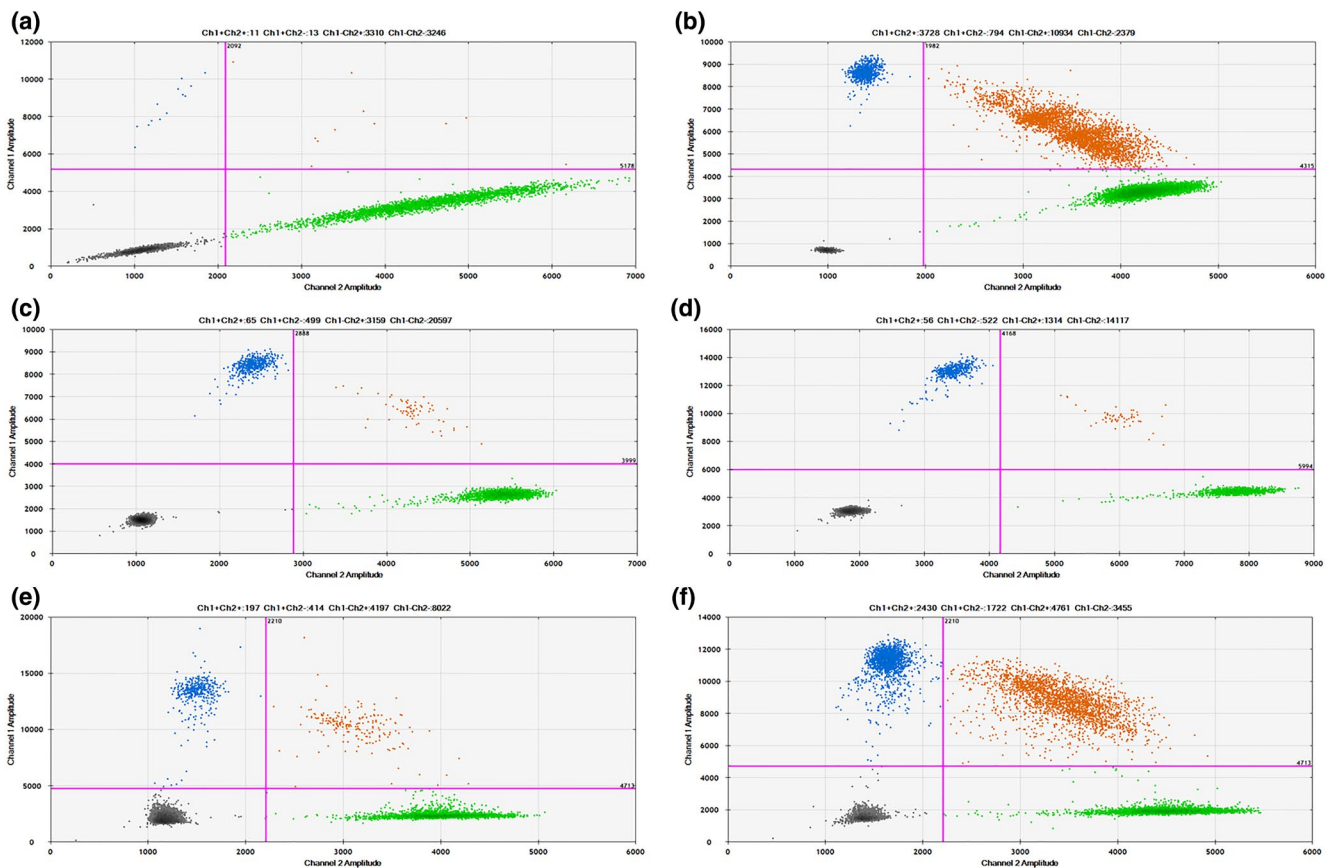


FIGURE 1 All droplets above the threshold intensity indicated by a pink line were scored as 'positives'. The green fluorescence signal represents wild-type. The blue fluorescence signal represents variant-type, and the orange fluorescence signal represents all positive droplets. Each droplet in a sample was plotted as a graph of fluorescence intensity versus droplet number. The A represents the allele frequency (AF) of *TSC2*: c.976-5G>A in the umbilical cord (0.72%, 24/3345), and B represents that in cardiac rhabdomyoma (CR) (23.57%, 4522/19184) in case 2. The C represents the AF of *TSC2*: c.894dupT in the umbilical cord (14.89%, 564/3788), and D represents that in CR (29.67%, 578/1948) in case 3. The E represents the AF of *TSC2*: c.3323_3350del in the umbilical cord (12.20%, 611/5005), and F represents that in CR (36.60%, 4152/11343) in case 4

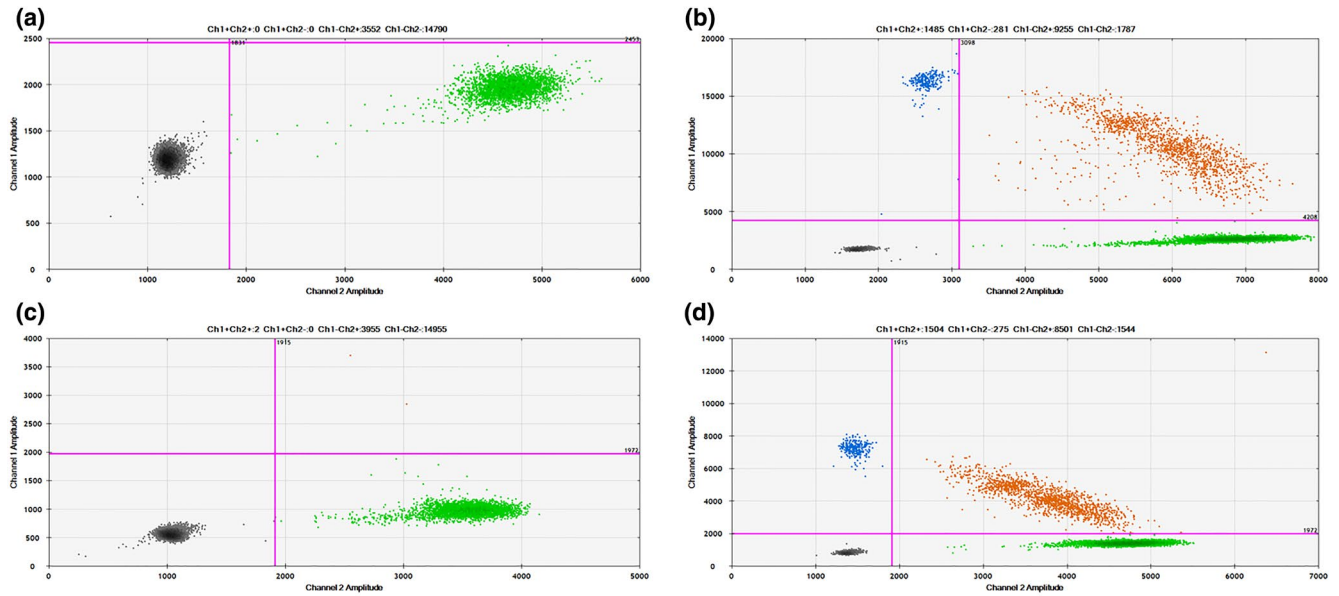


FIGURE 2 The A represents the AF of TSC2: c.475G>T in the umbilical cord (0, 0/3552), and B represents that in CR (14.12%, 1766/12506) in case 5. The C represents the AF of TSC2: c.3412C>T in the umbilical cord (0.05%, 2/3959), and the D represents that in CR (15.10%, 1779/11784) in case 5

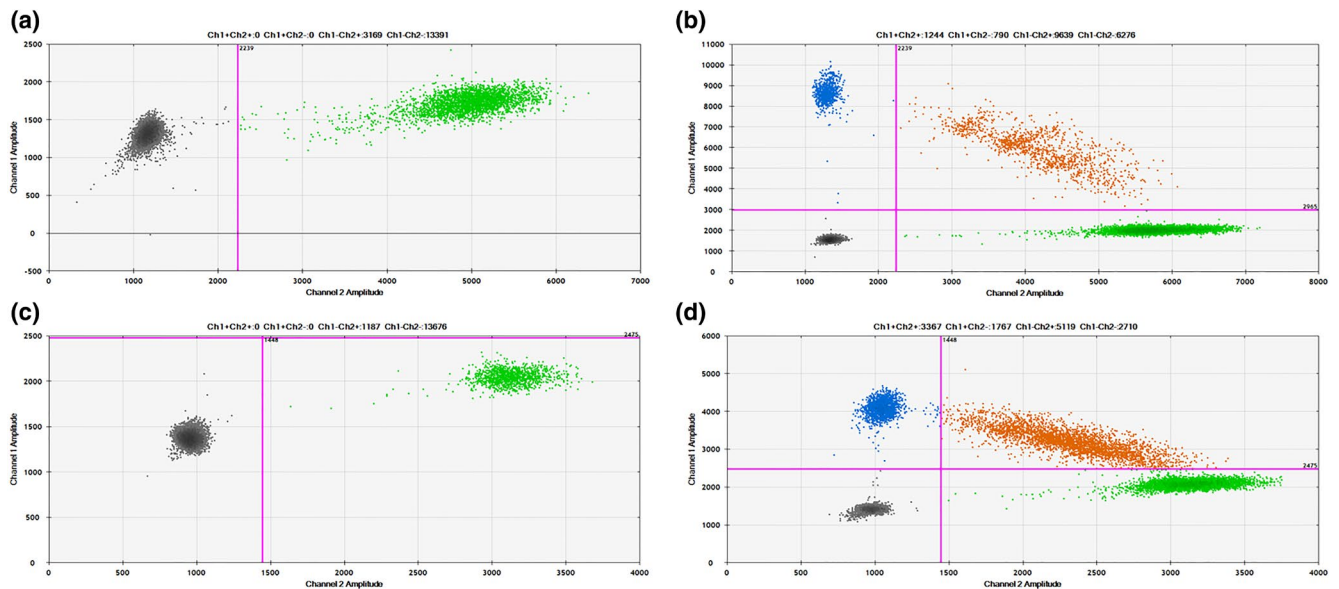


FIGURE 3 The A represents the AF of TSC2: c.4663-1G>A in the umbilical cord (0, 0/3169), and B represents that in CR (15.76%, 2034/12917) in case 1. The C represents the AF of TSC2: c.1831C>T in the umbilical cord (0, 0/1187), and D represents that in CR (37.69%, 5134/13620) in case 6

p.R786* *TSC1* variant at an AF of 4.86% (208/4277) in the blood and at 36.23% (892/2462) in the semen (Figure 5).

4 | DISCUSSION

Here we reported eight families of fetuses with CR, six of whom had been screened for *TSC1/TSC2* variants by

TSC1/TSC2 panel sequencing and MLPA, with no pathogenic variants identified. By analyzing umbilical cord tissues, CR tissues, and semen samples from two fathers with gonadal mosaicism, we were able to identify low-level and somatic mosaic variants in all six of these NMI fetuses. Two of the fetuses had inherited variants via paternal mosaicism, and both of these fathers exhibited low-level mosaicism and gonadal mosaic variants.

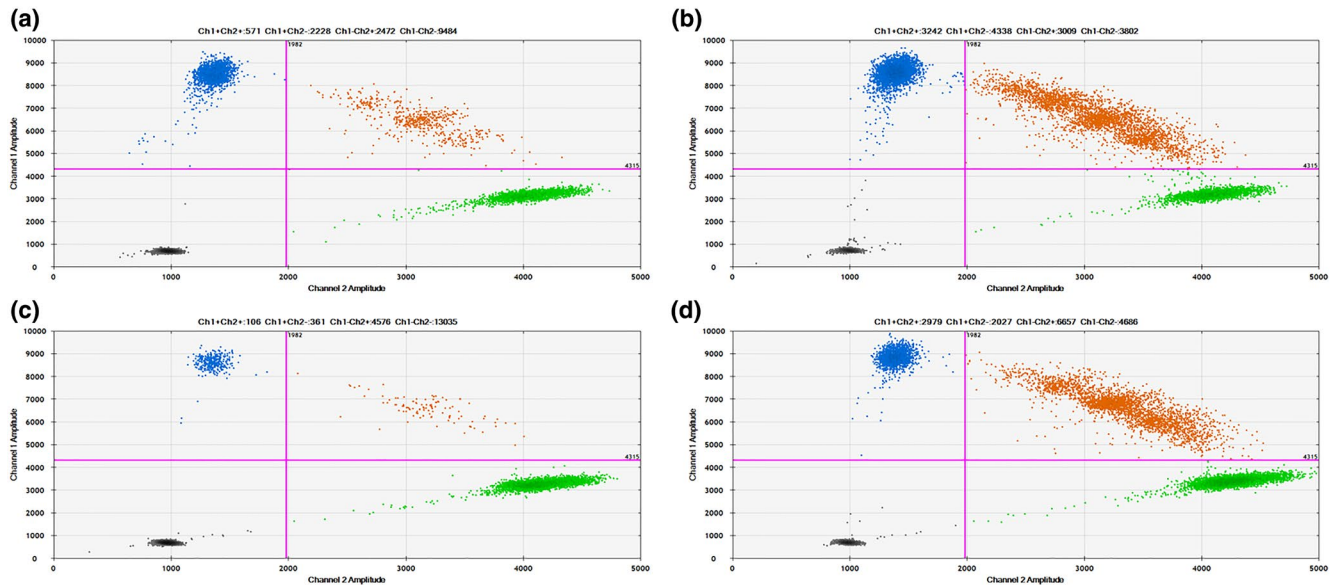


FIGURE 4 The A represents the AF of TSC2: c.976-5G>A in the umbilical cord (51.06%, 2799/5482), and B represents that in CR (54.80%, 7580/13831), and C represents that in paternal blood (9.07%, 467/5149), and D represents that in paternal semen (34.19%, 5006/14642)

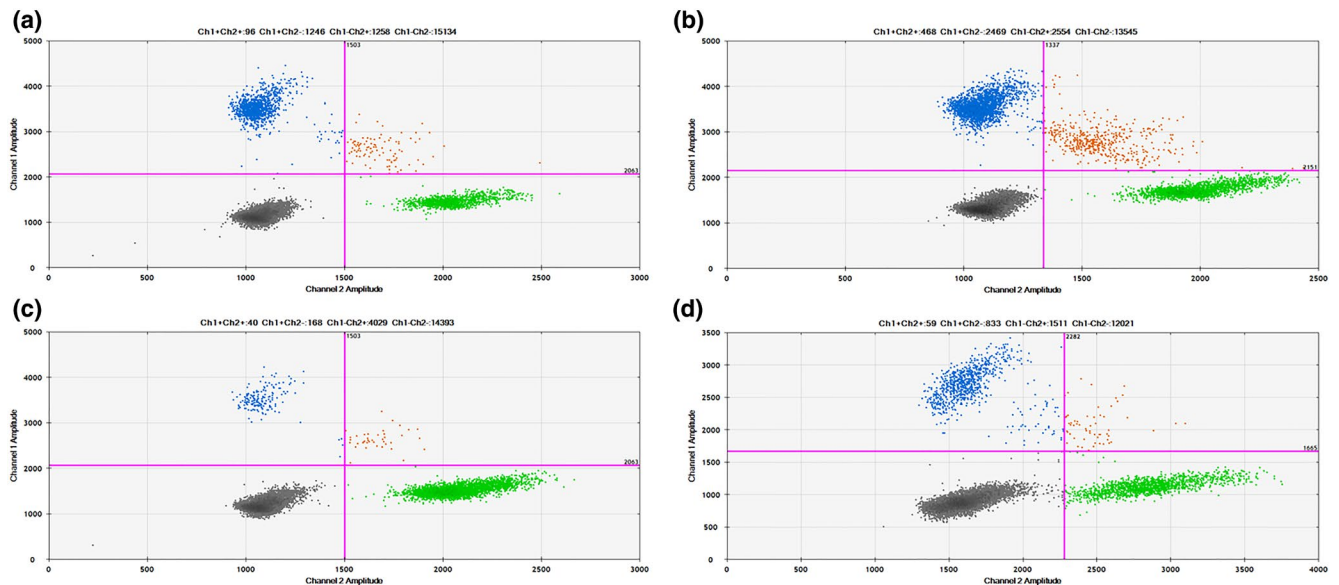


FIGURE 5 The A represents the AF of TSC1: c.2356C>T in the umbilical cord (49.78%, 1342/2696), and B represents that in CR (49.28%, 2397/5959), and C represents that in paternal blood (4.86%, 208/4277), and D represents that in paternal semen (36.23%, 892/2462)

4.1 | Mosaic variants in fetuses with CR

Low-level and somatic mosaic variants have previously been reported in patients with TSC (Nellist et al., 2015; Tyburczy et al., 2015). In our study, we detected low-level mosaic variants in umbilical cord tissue from four fetuses. AFs were significantly higher for variants detected in the CR tissue than for those detected in the umbilical cord tissue. Therefore, analyzing tumor tissue could help improve

the *TSC1/TSC2* variant detection rate, especially in NMI patients. Our findings suggest that NGS could be used for the prenatal diagnosis of fetuses with TSC carrying low-level mosaic variants.

We detected somatic *TSC1/TSC2* variants in CR tissue in two fetuses, similar to previous reports of angiofibroma and AML in patients with TSC (Badri et al., 2013; Carsillo et al., 2000). Recent studies have shown that AML and lymphangiomyomatosis (LAM) can arise

independently in patients without TSC (Badri et al., 2013; Carsillo et al., 2000; Qin et al., 2011). We suggest that fetal CR can also arise independently in fetuses without TSC, similar to the AML that occurs in patients who carry somatic *TSC1/TSC2* variants. Most independent AMLs and LAMs exhibit biallelic loss of *TSC1/TSC2*, and the somatic mosaic variants identified in CR tissue in this study were point variants (Cai et al., 2010; Qin et al., 2011). We cannot rule out the possibility that some of the cases included in our study carried extremely low-level mosaic variants that current sequencing technologies are not sensitive enough to detect. It is worth noting that low-level and somatic mosaic variants tend to be associated with milder clinical manifestations (Sampson et al., 1997; Verhoef et al., 1995).

4.2 | Second-hit variants in CR tissue

We identified two different variants in case 5, a situation that is referred to as having a second-hit variant. Second-hit variants have often been reported in patients with TSC. Studies have confirmed that second-hit variants in angiofibroma are related to sunlight-induced DNA damage (Tyburczy et al., 2014). Most second-hit variants in angiofibroma are point variants, and CC>TT accounts for 50% of these variants (Ikehata & Ono, 2011; Tyburczy et al., 2014). In AML, loss of heterozygosity is the most common second-hit variant, accounting for about 70%. Different second-hit variants can be present in different angiofibroma or AML tissues from the same patient with TSC (Ikehata & Ono, 2011; Tyburczy et al., 2014). Godava et al. reported a second-hit variant in CR that was a large deletion in *TSC2* (Godava et al., 2017). In our study, only one patient with CR exhibited a second-hit variant (1/8, 12.5%), in contrast to the percentage of patients with angiofibroma (14/17, 82.4%) or AML (10/32, 31.2%) who have been reported to carry second-hit variants (Giannikou et al., 2016; Tyburczy et al., 2014). This apparent discrepancy may be because MLPA was not used to analyze CR tissue in our study, so large deletions/duplications in CR tissue would not have been detected. This lower rate of second-hit variants could also be related to the origin and pathogenesis of CR tumors. Interestingly, Giannikou et al. found that second-hit variants were more common in subjects without TSC than in subjects with TSC (Giannikou et al., 2016). Thus, more research is needed to elucidate the mechanisms and characteristics of second-hit variants in CR.

4.3 | Paternal mosaicism

In this study, we detected low-level mosaic variants in two paternal blood samples. The father of case 7 was clinically

diagnosed with TSC, whereas the father of case 8 exhibited no TSC-related clinical manifestations. A previous study has described patients with TSC who carry low-level variants but do not exhibit TSC-related clinical manifestations (Nellist et al., 2015). In this study, both fathers with low-level mosaicism had gonadal mosaic variants, and the AFs of these variants in the semen were >30%, which was significantly higher than the AFs in the peripheral blood. We detected low-level mosaic variants in four fetuses in our study. However, previous studies have suggested that clinical manifestations in patients with low-level mosaic variants are milder than in those with heterozygous variants. We believe that the patients with low-level mosaic may combine with gonadal mosaic variants. Therefore, the detection of low-level mosaic variants could help provide more accurate fertility guidance to patients.

5 | CONCLUSION

The fetuses assessed in this study carried low-level and somatic mosaic variants, and CR tissue from one fetus exhibited a second-hit variant. Heterozygous gonadal variants can exist in patients with low-level mosaicism. Combining NGS with ddPCR improves the accuracy of prenatal TSC diagnosis.

6 | LIMITATIONS

One limitation of this study is that we did not take multiple samples from the same tissue or tumor in each fetus to verify the results. In addition, we did not perform MLPA analysis of CR tissue, so we were unable to confirm whether there were large deletions or duplications constituting second-hit variants in CR tissue.

ACKNOWLEDGMENTS

We thank all sonographers, pathologists, and participants for their valuable contributions. Besides, the authors would like to thank WuXiNextCODE and Sangon Biotech for promoting NGS and ddPCR. We thank Emily Crow, PhD, from Liwen Bianji (Edanz) (www.liwenbianji.cn/) for editing the English text of a draft of this manuscript.

CONFLICT OF INTERESTS

None declared.

AUTHOR CONTRIBUTIONS

S Wang and H Sun conceived the study, performed the statistical analysis and wrote down the manuscript; J Wang performed molecular analyses; X Gu and L Han performed clinical evaluations of patients; Y Wu, H Yan

performed case collection; H Zhang and Y He provided financial support the manuscript.

ETHICS STATEMENT

The institutional committee approved this study on human research (2018050X).

DATA AVAILABILITY STATEMENT

The data are available.

ORCID

Siyu Wang  <https://orcid.org/0000-0001-9152-451X>

Hairui Sun  <https://orcid.org/0000-0002-5868-237X>

REFERENCES

- Au, K. S., Rodriguez, J. A., Finch, J. L., Volcik, K. A., Roach, E. S., Delgado, M. R., Rodriguez, E. Jr, & Northrup, H. (1998). Germline mutational analysis of the TSC2 gene in 90 tuberous-sclerosis patients. *American Journal of Human Genetics*, *62*, 286–294. <https://doi.org/10.1086/301705>
- Badri, K. R., Gao, L., Hyjek, E., Schuger, N., Schuger, L., Qin, W., Chekaluk, Y., Kwiatkowski, D. J., & Zhe, X. (2013). Exonic variants of TSC2/TSC1 are common but not seen in all sporadic pulmonary lymphangiomyomatosis. *American Journal of Respiratory and Critical Care Medicine*, *187*, 663–665.
- Cai, X., Pacheco-Rodriguez, G., Fan, Q. Y., Haughey, M., Samsel, L., El-Chemaly, S., Wu, H. P., McCoy, J. P., Steagall, W. K., Lin, J. P., Darling, T. N., & Moss, J. (2010). Phenotypic characterization of disseminated cells with TSC2 loss of heterozygosity in patients with lymphangiomyomatosis. *American Journal of Respiratory and Critical Care Medicine*, *182*, 1410–1418.
- Camposano, S. E., Greenberg, E., Kwiatkowski, D. J., & Thiele, E. A. (2009). Distinct clinical characteristics of tuberous sclerosis complex patients with no variant identified. *Annals of Human Genetics*, *73*, 141–146.
- Carsillo, T., Astrinidis, A., & Henske, E. P. (2000). Mutations in the tuberous sclerosis complex gene TSC2 are a cause of sporadic pulmonary lymphangiomyomatosis. *Proceedings of the National Academy of Sciences of the United States of America*, *97*, 6085–6090.
- Chen, J., Wang, J., Sun, H., Gu, X., Hao, X., Fu, Y., Zhang, Y., Liu, X., Zhang, H., Han, L., & He, Y. (2019). Fetal cardiac tumor: Echocardiography, clinical outcome and genetic analysis in 53 cases. *Ultrasound in Obstetrics and Gynecology*, *54*, 103–109. <https://doi.org/10.1002/uog.19108>
- DiMario, F. J., Sahin, M., & Ebrahimi-Fakhari, D. (2015). Tuberous sclerosis complex. *Pediatric Clinics of North America*, *62*, 633–648. <https://doi.org/10.1016/j.pcl.2015.03.005>
- European Chromosome 16 Tuberous Sclerosis C. (1993). Identification and characterization of the tuberous sclerosis gene on chromosome 16. *Cell*, *75*, 1305–1315.
- Giannikou, K., Malinowska, I. A., Pugh, T. J., Yan, R., Tseng, Y. Y., Oh, C., Kim, J., Tyburczy, M. E., Chekaluk, Y., Liu, Y., & Alesi, N. (2016). Whole exome sequencing identifies TSC1/TSC2 bi-allelic loss as the primary and sufficient driver event for renal angiomyolipoma development. *PLoS Genetics*, *12*, e1006242.
- Godava, M., Filipova, H., Dubrava, L., Vrtel, R., Michalkova, K., Janikova, M., Bakaj-Zbrozkova, L., & Navratil, J. (2017). Single giant mediastinal rhabdomyoma as a sole manifestation of TSC in foetus. *Biomedical Papers of the Medical Faculty of the University Palacky, Olomouc, Czechoslovakia*, *161*(3), 326–329. <https://doi.org/10.5507/bp.2017.023>
- Gu, X., Han, L., Chen, J., Wang, J., Hao, X., Zhang, Y., Zhang, J., Ge, S., & He, Y. (2018). Antenatal screening and diagnosis of tuberous sclerosis complex by fetal echocardiography and targeted genomic sequencing. *Medicine (Baltimore)*, *97*, e112. <https://doi.org/10.1097/MD.00000000000010112>
- Henske, E. P., Jozwiak, S., Kingswood, J. C., Sampson, J. R., & Thiele, E. A. (2016). Tuberous sclerosis complex. *Nature Reviews Disease Primers*, *2*, 16035. <https://doi.org/10.1038/nrdp.2016.35>
- Ikehata, H., & Ono, T. (2011). The mechanisms of UV mutagenesis. *Journal of Radiation Research*, *52*, 115–125.
- International Society of Ultrasound in Obstetrics and Gynecology, Carvalho, J. S., Allan, L. D., Chaoui, R., Copel, J. A., DeVore, G. R., Hecher, K., Lee, W., Munoz, H., Paladini, D., Tutschek, B., & Yagel, S. (2013). ISUOG Practice Guidelines (updated): Sonographic screening examination of the fetal heart. *Ultrasound in Obstetrics and Gynecology*, *41*, 348–359.
- Jones, A. C., Shyamsundar, M. M., Thomas, M. W., Maynard, J., Idziaszczyk, S., Tomkins, S., Sampson, J. R., & Cheadle, J. P. (1999). Comprehensive mutation analysis of TSC1 and TSC2 and phenotypic correlations in 150 families with tuberous sclerosis. *American Journal of Human Genetics*, *64*, 1305–1315. <https://doi.org/10.1086/302381>
- Jozwiak, S., & Kotulska, K. (2006). Are all prenatally diagnosed multiple cardiac rhabdomyomas a sign of tuberous sclerosis? *Prenatal Diagnosis*, *26*, 867–869. <https://doi.org/10.1002/pd.1506>
- Lam, H. C., Nijmeh, J., & Henske, E. P. (2017). New developments in the genetics and pathogenesis of tumours in tuberous sclerosis complex. *The Journal of Pathology*, *241*, 219–225.
- Nellist, M., Brouwer, R. W., Kockx, C. E., van Veghel-Plandsoen, M., Withagen-Hermans, C., Prins-Bakker, L., Hoogeveen-Westerveld, M., Mrsic, A., van den Berg, M. M., Koopmans, A. E., de Wit, M. C., Jansen, F. E., Maat-Kievit, A. J., van den Ouweland, A., Halley, D., de Klein, A., & van IJcken, W. F. (2015). Targeted Next Generation Sequencing reveals previously unidentified TSC1 and TSC2 variants. *BMC Medical Genetics*, *16*, 10.
- Niida, Y., Lawrence-Smith, N., Banwell, A., Hammer, E., Lewis, J., Beauchamp, R. L., Sims, K., Ramesh, V., & Ozelius, L. (1999). Analysis of both TSC1 and TSC2 for germline mutations in 126 unrelated patients with tuberous sclerosis. *Human Mutation*, *14*, 412–422. [https://doi.org/10.1002/\(SICI\)1098-1004\(199911\)14:5<412::AID-HUMU7>3.0.CO;2-K](https://doi.org/10.1002/(SICI)1098-1004(199911)14:5<412::AID-HUMU7>3.0.CO;2-K)
- Northrup, H., & Krueger, D. A. (2013). Tuberous sclerosis complex diagnostic criteria update: Recommendations of the 2012 International Tuberous Sclerosis Complex Consensus Conference. *Pediatric Neurology*, *49*, 243–254.
- Pavlicek, J., Klaskova, E., Kapralova, S., Prochazka, M., Vrtel, R., Gruszka, T., & Kacerovsky, M. (2021). Fetal heart rhabdomyomatosis: A single-center experience. *The Journal of Maternal-Fetal & Neonatal Medicine*, *34*(5), 701–707. <https://doi.org/10.1080/14767058.2019.1613365>
- Qin, W., Bajaj, V., Malinowska, I., Lu, X., MacConaill, L., Wu, C. L., & Kwiatkowski, D. J. (2011). Angiomyolipoma have common

- variants in TSC2 but no other common genetic events. *PLoS One*, *6*, e24919.
- Richards, S., Aziz, N., Bale, S., Bick, D., Das, S., Gastier-Foster, J., Grody, W. W., Hegde, M., Lyon, E., Spector, E., Voelkerding, K., & Rehm, H. L.; ACMG Laboratory Quality Assurance Committee. (2015). Standards and guidelines for the interpretation of sequence variants: A joint consensus recommendation of the American College of Medical Genetics and Genomics and the Association for Molecular Pathology. *Genetics in Medicine*, *17*, 405–424. <https://doi.org/10.1038/gim.2015.30>
- Sampson, J. R., Maheshwar, M. M., Aspinwall, R., Thompson, P., Cheadle, J. P., Ravine, D., Roy, S., Haan, E., Bernstein, J., & Harris, P. C. (1997). Renal cystic disease in tuberous sclerosis: Role of the polycystic kidney disease 1 gene. *American Journal of Human Genetics*, *61*, 843–851.
- Tyburczy, M. E., Dies, K. A., Glass, J., Camposano, S., Chekaluk, Y., Thorner, A. R., Lin, L., Krueger, D., Franz, D. N., Thiele, E. A., Sahin, M., & Kwiatkowski, D. J. (2015). Mosaic and intronic variants in TSC1/TSC2 explain the majority of TSC patients with no variant identified by conventional testing. *PLoS Genetics*, *11*, e1005637.
- Tyburczy, M. E., Wang, J. A., Li, S., Thangapazham, R., Chekaluk, Y., Moss, J., Kwiatkowski, D. J., & Darling, T. N. (2014). Sun exposure causes somatic second-hit variants and angiofibroma development in tuberous sclerosis complex. *Human Molecular Genetics*, *23*, 2023–2029.
- van Slegtenhorst, M., de Hoogt, R., Hermans, C., Nellist, M., Janssen, B., Verhoef, S., Lindhout, D., van den Ouweland, A., Halley, D., Young, J., Burley, M., Jeremiah, S., Woodward, K., Nahmias, J., Fox, M., Ekong, R., Osborne, J., Wolfe, J., Povey, S., ... Kwiatkowski, D. J. (1997). Identification of the tuberous sclerosis gene TSC1 on chromosome 9q34. *Science*, *277*, 805–808. <https://doi.org/10.1126/science.277.5327.805>
- Verhoef, S., Vrtel, R., van Essen, T., Bakker, L., Sikkens, E., Halley, D., Lindhout, D., & van den Ouweland, A. (1995). Somatic mosaicism and clinical variation in tuberous sclerosis complex. *The Lancet*, *345*, 202. [https://doi.org/10.1016/S0140-6736\(95\)90213-9](https://doi.org/10.1016/S0140-6736(95)90213-9)

SUPPORTING INFORMATION

Additional Supporting Information may be found online in the Supporting Information section.

How to cite this article: Wang, S., Sun, H., Wang, J., Gu, X., Han, L., Wu, Y., Yan, H., Han, L., Zhang, H., & He, Y. (2021). Detection of *TSC1/TSC2* mosaic variants in patients with cardiac rhabdomyoma and tuberous sclerosis complex by hybrid-capture next-generation sequencing. *Molecular Genetics & Genomic Medicine*, *9*, e1802. <https://doi.org/10.1002/mgg3.1802>